# *VOYAGER 2* OBSERVATIONS OF PLASMAS AND FLOWS OUT TO 104 AU

J. D. Richardson[1] and R. B. Decker[2]

[1] Kavli Center for Astrophysics and Space Science, Massachusetts Institute of Technology, Cambridge, MA 02139, USA; jdr@space.mit.edu
[2] Applied Physics Laboratory, Johns Hopkins University, Laurel, MD, USA; robert.decker@apljhu.edu

## ABSTRACT

*Voyager 2* has crossed through 20 AU of the heliosheath; assuming the same heliosheath thickness as at *Voyager 1*, it is now two-thirds of the way to the heliopause. The plasma data are generally of good quality, although the increasing flow angle of the plasma makes analysis more difficult. The average plasma speed has remained constant but the flow angles have increased to almost $60°$ in the RT plane and to almost $30°$ in the RN plane. The average density and thermal speed have been constant since a density increase observed in 2011. Comparison of *V2* plasma flows derived from plasma science experiment (PLS) data and Low Energy Charged Particle (LECP) proton anisotropies give good agreement except when heavy ion contributions or non-convective proton anisotropies are observed in the LECP data.

*Key words:* solar wind – Sun: heliosphere

*Online-only material:* color figures

## 1. INTRODUCTION

In the beginning of 2014 *Voyager 2* (*V2*) was at 104 AU and had traversed 20 AU of the heliosheath. *Voyager 1* (*V1*) crossed a boundary in 2012 at 124 AU, characterized by an increase in magnetic field strength and cosmic ray intensities and a dropout of the energetic particles (Burlaga et al. 2013a; Webber & McDonald 2013; Krimigis et al. 2013; Stone et al. 2013). At first this boundary was thought to indicate the beginning of a transition layer inside the heliopause. However, plasma wave data show that the plasma density after this boundary is comparable to that expected in the interstellar medium, so the current consensus is that this boundary was the heliopause and *V1* is now in the interstellar medium (Gurnett et al. 2013; Burlaga et al. 2013b; Webber & McDonald 2013). This view is not universally held; some suggest that the boundary layer hypothesis still fits the data and *V1* is still inside the heliopause (Fisk & Gloeckler 2013). In either case, this boundary is 30 AU beyond the termination shock (TS) crossing. If the heliosheath width were the same in both the V1 and V2 directions, V2 would cross the boundary in early 2017.

*Voyager 1* does not have a working plasma instrument, so *V2* will make the first plasma measurements of the regions near the heliopause and in the interstellar medium. Low-energy proton anisotropies were used to derive plasma flows at *V1* (Gleeson & Axford 1968; Decker et al. 2005, 2010) but densities and temperatures can usually not be determined. The exceptions were the two regions after the heliopause where plasma emissions were observed that allowed the density to be derived (Gurnett et al. 2013). Comparison of the velocities shows a very different flow structure in the *V1* and *V2* directions (Richardson & Wang 2012). This paper presents *V2* heliosheath plasma data out to 104 AU, compares these data to the *V1* observations and to *V2* flows derived from Low Energy Charged Particle (LECP) data, and discusses the implications of these results.

## 2. THE DATA

A detailed description of the Voyager Plasma Experiment (PLS) and the data analysis are given elsewhere (Bridge et al.

1977; Richardson & Wang 2012). The PLS instrument measures ion currents in four Faraday cups, three (A, B, and C) oriented about a central axis pointed toward Earth and the fourth (D) pointed perpendicular to this axis. The acceptance angle of each cup is constant for flows from 0 to $45°$ from the cup normal direction; the instrument response decreases roughly linearly to zero from 45 to $60°$. Thus, flows with angles larger than about $60°$ from the detector normal are not observed by that detector. To find the vector velocity requires data in three of the four cups. When this condition is met, the measured currents are fit to convected isotropic proton Maxwellian distributions to determine the proton velocity, density, and temperature. These distributions generally fit the data well, although the observed currents are close to the instrument threshold so that alpha particles and low-density tails to the distribution could be present but not observed.

Figure 1 shows a set of spectra chosen at a time when the instrument observed currents in all four Faraday cups; more typically currents are observed in only three of the cups (the minimum for performing the analysis). The histogram shows the observed currents in femtoamps ($10^{-15}$ A) plotted versus channel number, a roughly logarithmic energy scale ranging from 10 eV to 5950 eV. The A and B cups look closest to the flow direction and observe the largest currents. All cups suffered radiation damage at Jupiter resulting in the nonconstant noise observed in the higher energy channels. Careful selection of the channels to fit is key for the data analysis. The curves show the simulated currents produced using a proton Maxwellian distribution as input. The fit values for the three components of velocity ($V_R$, $V_T$, $V_N$), proton density ($N$), and proton thermal speed ($W_{TH}$) with $1\sigma$ errors from the fits are listed below the spectra. (The RTN system has R radially outward, T in the plane of the solar equator and positive in the direction of solar rotation, and N completes a right-handed system.) The fit shown here is a typical match to the data.

Figure 2 shows each individual 192 s data point and 25 day (1 solar rotation) running averages of $V_R$, $V_T$, $V_N$, $W_{TH}$, and N. $V_R$ is shown in the top panel; expectations are that $V_R$ should decrease across the heliosheath and approach zero near the heliopause. The *V1* data show a nearly monotonic decrease of $V_R$ across the heliosheath from 70 to 0 km s$^{-1}$ from 2005 to 2010
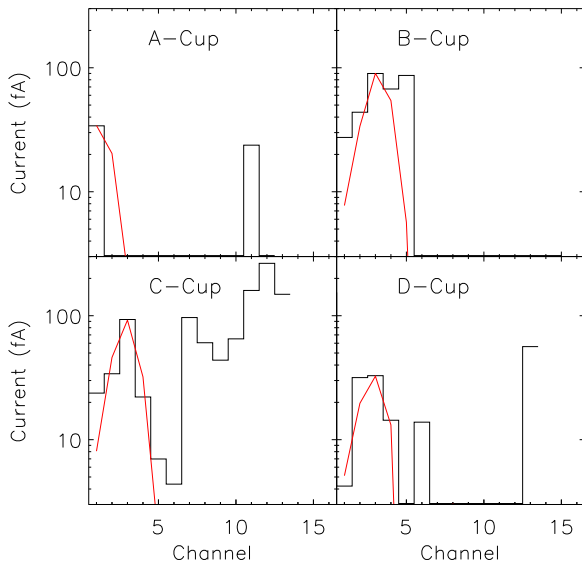
**Figure 1.** Set of PLS current vs. energy spectra from 2014, day 90, hr 4, minute 57:46 at 104.4 AU. The histogram shows the current in fA ($10^{-15}$) and the curve shows the fit to the data. For these spectra the fit parameters and $1\sigma$ uncertainties are $V_R = 120 \pm 3$ km s$^{-1}$, $V_T = 115 \pm 8$ km s$^{-1}$, $V_N = -11 \pm 7$ km s$^{-1}$, $N = 0.0016 \pm 0.0002$ cm$^{-3}$, and $W_{TH} = 29 \pm 4$ km s$^{-1}$. Noise is evident in some of the upper energy channels.

(A color version of this figure is available in the online journal.)

(Krimigis et al. 2011). At *V2*, $V_R$ decreased across the heliosheath but very slowly. Over the past two years the average $V_R$ varied from 80 to 120 km s$^{-1}$, with an average value of 96 km s$^{-1}$. The *V1* $V_R$ values were much lower throughout the heliosheath (Decker et al. 2005; Krimigis et al. 2011). A simple linear fit to the *V2* $V_R$ data gives a speed decrease of 8 km s$^{-1}$ yr$^{-1}$, at which rate it would take over 10 years for $V_R$ to go to zero.

The second and third panels of Figure 2 show $V_T$ and $V_N$ in the same format as $V_R$. The nonradial components of velocity are expected to increase as the flow turns and moves tailward. Such an increase was not observed at *V1*, where $V_T$ remained almost constant from the TS to the stagnation region and $V_N$ decreased as $V_R$ decreased. At *V2* both $V_T$ and $V_N$ increase across the heliosheath. After the TS in 2007 $V_T$ averaged 43 km s$^{-1}$; for the last two years the average was 93 km s$^{-1}$. The apparent flattening of the $V_T$ curve after 2012 is probably an instrument selection effect, with large $V_T$ leading to flow angles above the instrument threshold. $V_N$ increased from 22 km s$^{-1}$ in 2007 to 68 km s$^{-1}$ in 2013, but is one-third smaller than $V_T$ and thus not affected by the instrument response. We note that $V_T$ and $V_N$ are correlated after mid 2011, increasing and decreasing in unison for several months at a time.

The fourth panel shows the density. The density decreased by a factor of two in 2008, then recovered in Richardson & Wang (2012). Since this increase the average density has remained fairly constant with a value of 0.0018 cm$^{-3}$ in 2013, comparable to the density of 0.0021 cm$^{-3}$ observed in 2007 after the TS. The 25 day average values have varied significantly over the past two years, from 0.0015 to 0.0025 cm$^{-3}$. The bottom panel shows $W_{TH}$, which has not varied greatly since 2009 and in 2013 averaged 28.8 km s$^{-1}$, corresponding to a temperature of 50,000 K.

Next we consider the typical uncertainties in these values. Figure 3 shows 101 point running averages of the ratio of x$V_R/V_R$, x$N/N$, and x$W_{TH}/W_{TH}$ (where x* is the $1\sigma$ error of *)
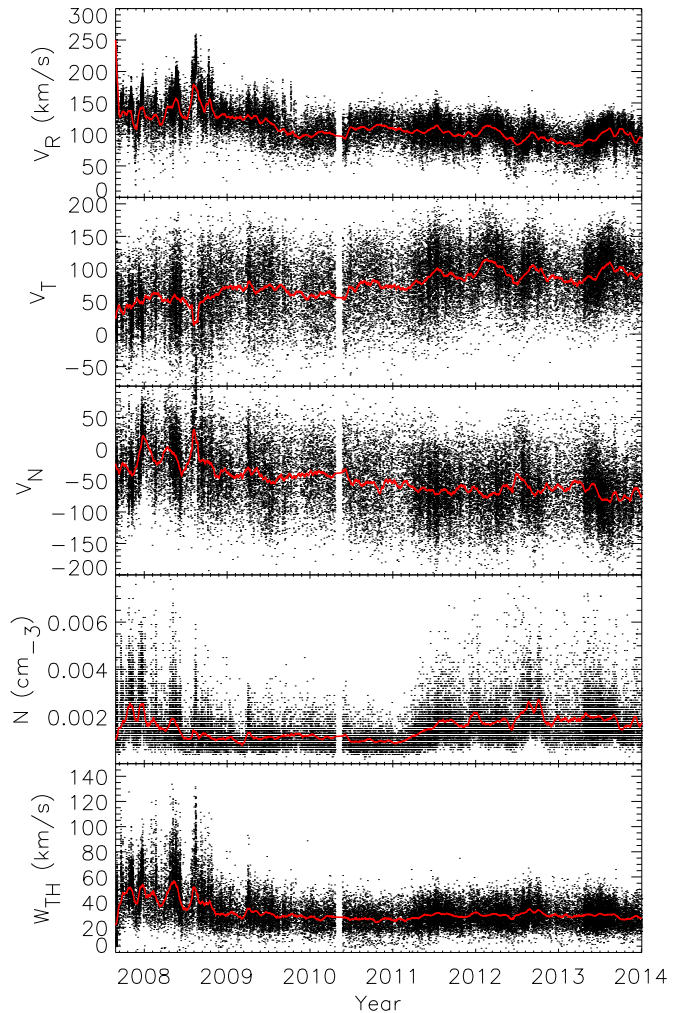


**Figure 2.** Individual data points and 25 day running averages of the plasma parameters derived by fitting the data to convected isotropic proton Maxwellians.

(A color version of this figure is available in the online journal.)

and of the errors in $V_T$ and $V_N$ in km s$^{-1}$. $V_R$ is the best determined parameter since the flow in the $R$-direction is directly into three of the cups; the average uncertainty is 8.4%. The average density uncertainty is about 25%, with higher values before and lower after the density increase which occurred in 2011. The increase in density improves the signal-to-noise ratio in the measured currents and decreases the uncertainties. This trend is very clear in the thermal speed uncertainties as well. These $1\sigma$ errors average 30.7%, but are 39% in the lower density region from 2009 to 2010 and 26% in the higher density region after 2011. These fairly large uncertainties derive from the low-resolution energy channels used to measure the low currents in the heliosheath ($\Delta E/E = 29\%$) and from the low densities. For $V_T$ and $V_N$ the uncertainties are shown in km s$^{-1}$; for $V_T$ they are about 30 km s$^{-1}$, 35 km s$^{-1}$ in the lower density region, and 27 km s$^{-1}$ after 2011. For $V_N$, they are somewhat less, 23 km s$^{-1}$ in the low density region, 16 km s$^{-1}$ after 2011, and average 20 km s$^{-1}$ over the whole heliosheath.

Figure 4 shows parameters derived from the fit parameters, the magnitude of *V*, and the flow angles in the RT and RN planes. $|V|$ is remarkable in that the average value has not changed as *V2* has moved through the heliosheath. $|V|$ ranges from 125 to 175 km s$^{-1}$, with speed excursions typically lasting several months, but the average value has stayed at 146 km s$^{-1}$. The
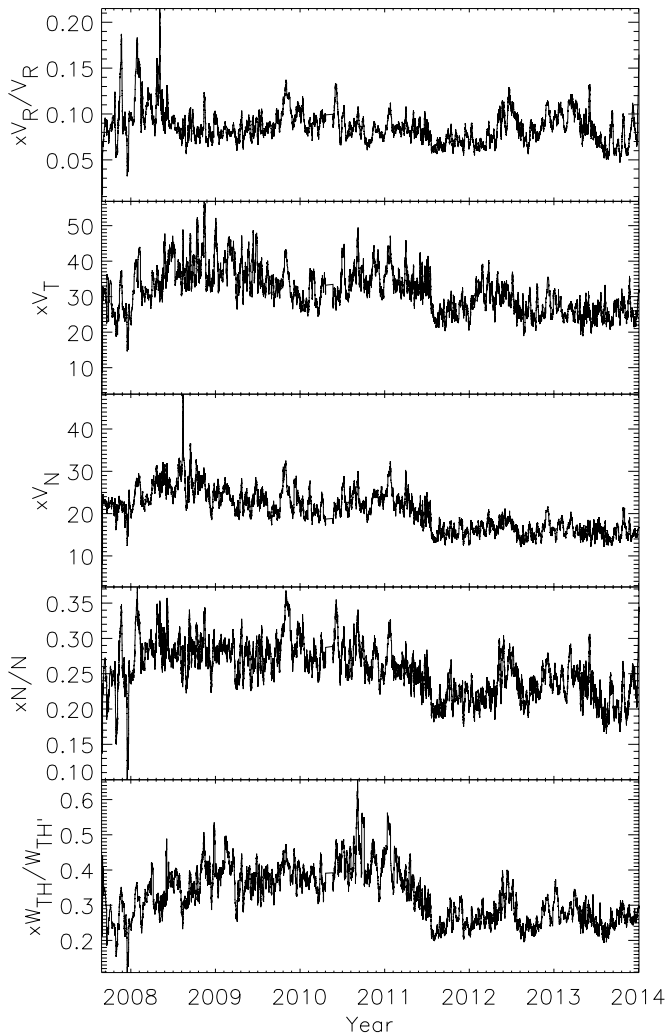
**Figure 3.** Relative $1\sigma$ errors for $V_R$, N, and $W_{TH}$ and $1\sigma$ errors in $V_T$ and $V_N$.



**Figure 4.** Individual data points and 25 day running averages of the speed and flow angles of the heliosheath plasma. The diamonds in the RT angle plot show the angles corrected for the instrument response.

(A color version of this figure is available in the online journal.)

decrease in $V_R$ is compensated for by increases in $V_T$ and $V_N$. A constant $|V|$ is not predicted by models and is very different from $V1$ observations which show a decrease in $|V|$ from about $100\ \mathrm{km\ s^{-1}}$ in 2005 to near zero in 2010.

The bottom two panels of Figure 4 show the flow angles. The RT angle shows a clear cutoff in values between $55°$ and $60°$ due to the instrument response. The few points with larger angles are from spectra with signal in the side-looking D-cup or with unusual plasma characteristics (such as a large thermal speed) which allow currents to be observed in the three sunward-looking detectors. The diamonds show the corrected RT angles, discussed below. After the TS in 2007 the average RN angle is $-9°$; the average increases to $-27°$ in 2013. The RN angles are not as large as the RT angles; RN is $-27°$ in 2013 whereas the corrected RT values are $58°$. The distribution of RN angles is only slightly affected by the instrument cutoff. The profiles of both RT and RN angles are relatively smooth compared to those of $V_R$, $V_T$, and $V_T$; the correlated variations in the speed components result in little change in the flow direction.

Figure 4 shows that the RT angles are affected by the instrument response. The heliosheath is a region which is highly variable (Richardson 2011; Burlaga & Ness 2009) on timescales of tens of minutes so that a distribution of plasma values is observed. These distributions are remarkably well fit by Gaussian distributions. Figure 5 shows the distribution of
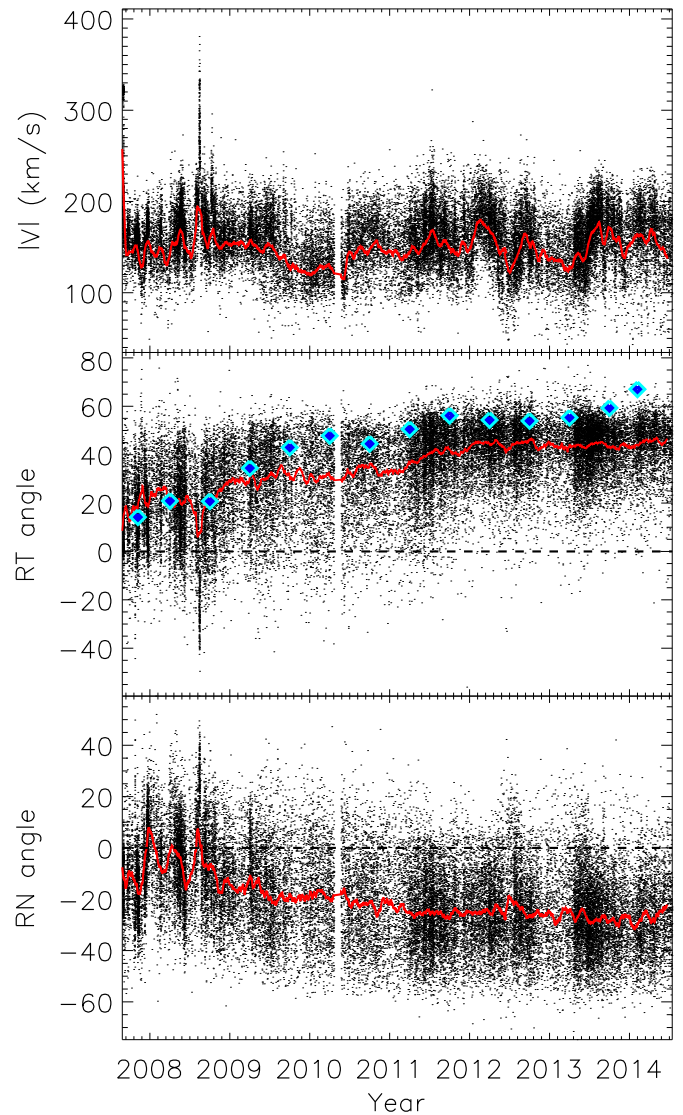
measured angles in 2007, 2010, and 2013. The distributions are Gaussian in each case out to $50°$, where the instrumental cutoff becomes important. If we assume the RT distributions remain Gaussian, we can fit the observations above the cutoff and determine the full distribution, which yields the average flow angle. A full distribution is needed to determine the corrections; we calculate a new correction every six months. For the RT angle, the corrected average value for the second half of 2013 is $59°$, compared to an average from the measured spectra of $44°$. So, the correction is significant. If we do the same calculation for the RN angle the correction is only $1.7°$.

From Figure 5 it is clear that in recent years the plasma instrument data cannot be used to determine plasma parameters for a large proportion of the plasma spectra. An obvious concern is that removing all high flow-angle plasma from the analysis could bias the calculation of the other plasma parameters. This would be the case if the other plasma parameters were correlated with flow angle. We have looked at the dependence of the speed components, density, and thermal speed of RT and find no significant correlation. Thus the values we show in the plots
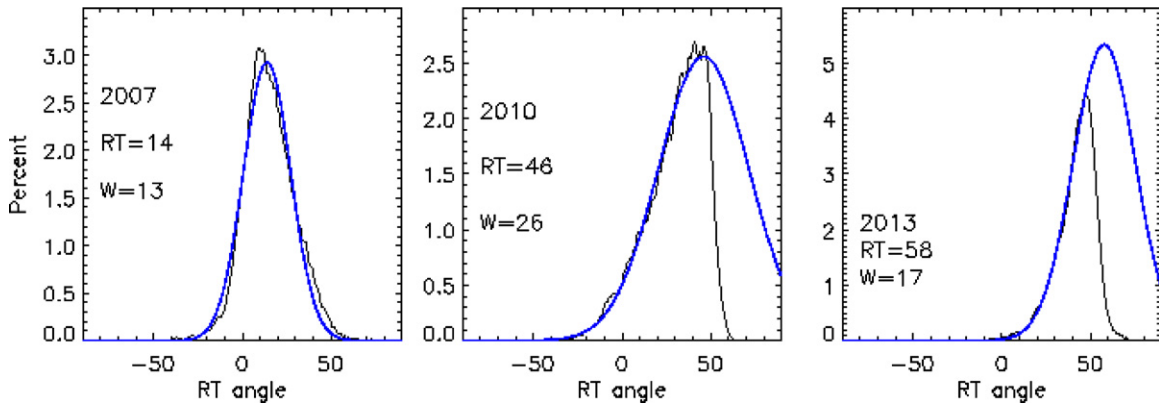
**Figure 5.** Distribution of angles in the RT plane in 2007, 2010, and 2013 (white lines) and Gaussian fits to these distributions (blue lines). The average RT angle and the width of the distribution, both from the Gaussian fits, are given in each panel.

(A color version of this figure is available in the online journal.)

above need no correction except for $V_T$ and the RT angle. The spectra with large RT angles, $>55°$, do have larger average densities and thermal speeds than those with lower RT angles; high angle flows with higher densities and thermal speeds are easier to observe.

## 3. DISCUSSION

As mentioned earlier, the flows observed by *V2* are very different from those observed by *V1*. They are also derived in different ways, by fitting the plasma data for *V2* but by using Compton–Getting analysis on the low-energy particle data for *V1*. The question then is whether the differences in flow are real or due to the different measurement techniques. One way to address this question is to compare the speeds derived from these two methods at *V2*. Figure 6 compares the values of $V_R$, $V_T$, and $V_{RT}$ ($\sqrt{V_R^2 + V_T^2}$) derived from the plasma data and from the LECP 28–43 keV ion (generally proton) angular data using a linear Compton–Getting analysis. The Compton–Getting analysis assumes the ion composition is known and that the observed anisotropies arise from the convective flow. The $V_R$ panel shows that the values match fairly well after the TS, then LECP finds much larger values from 2009.3–2010.5 (period A in the $V_R$ panel). The values match fairly well after that, except for a few times when the LECP $V_R$ values are higher from 2012.7–2013.3 and near 2013.7. The $V_T$ profiles look similar, with increasing values through the heliosheath, except from 2012.7–2013.3 (period B in the $V_T$ panel). The differences in $V_R$ during 2009.3–2010.5 are most likely due to pickup oxygen ions. The ion detector used measures total energy, so the 28–43 keV proton channel will also measure 4–7 keV oxygen ions (Krimigis et al. 1981). The Compton–Getting analysis used to derive flow estimates in Figure 6 assumed protons, which would overestimate the predicted convection speed if oxygen were present because of the higher speed of protons relative to that of pickup oxygen ions. It is unclear why these heavy ions are prevalent at *V2* during 2009.3–2010.5. However, pickup oxygen ions have been measured by the *V1* and V2 LECP low-energy ion channels in high speed solar wind (Decker et al. 2003). A small energy boost at the termination shock would enable pickup oxygen detection by LECP in the low speed heliosheath flow. In the region from 2012.7 to 2013.3, ions from at least 28 keV to several MeV are streaming along the magnetic field, so the observed isotropies are not purely from flow convection and the Compton–Getting
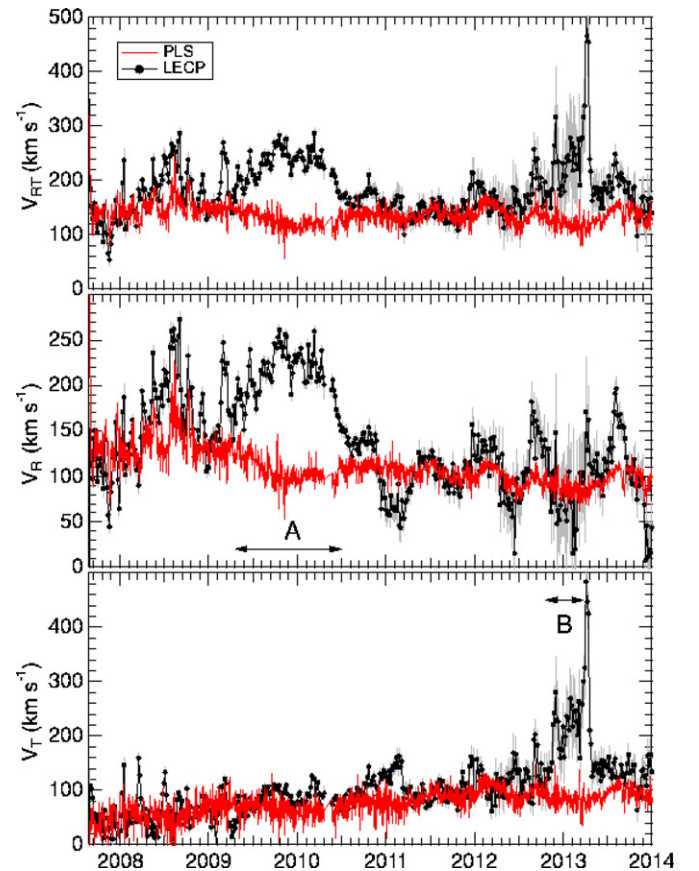


**Figure 6.** Comparison of V2 PLS measurements of the flow speed in the RT plane $V_{RT}$ (top), $V_R$ (middle), and $V_T$ (bottom), with the same quantities determined from Compton–Getting analysis of V2 LECP 28–43 keV ion angular data. The PLS data are daily averages and the LECP points are five-day averages.

(A color version of this figure is available in the online journal.)

analysis is unreliable. Where PLS and LECP speeds can both be reliably determined the values are comparable. Both LECP and PLS observe much higher values of $V_R$ than LECP observed at *V1* and a very slow decrease in $V_R$ across the heliosheath. Both PLS and LECP observe an increase in $V_T$ across the heliosheath, which is again very different from the constant low-speed $V_T$ observed at *V1*. We note that where LECP and PLS disagree the LECP values are larger than the PLS values; similar problems with the Compton–Getting analysis at *V1* would also give larger

values of $V_T$ and $V_R$, not lower values as observed. The data thus are consistent, with the flow speeds in the *V1* and *V2* directions actually being very different; this difference does not appear to be an instrumental effect.

We note that some models of the heliosphere suggest that the speed fluctuations will increase with distance (Fisk & Gloeckler 2009). Neither the individual points or running averages in Figure 2 show any indication of an increase in fluctuations. The relative standard deviations of the velocity components across the heliosheath show no increase.

Models of the heliospheric interaction with the interstellar medium have so far not succeeded in simulating both the *V1* and *V2* speed profiles. Two recently published simulations of plasma parameters are from Pogorelov et al. (2013) and Provornikova et al. (2014). Pogorelov et al. (2013) use *Ulysses* data as input to construct a 3D model, and thus can simulate the heliosphere only until 2011. This simulation matches the TS locations well. In the heliosheath the model matches the *V2* $V_R$ data but gives much greater values in the *V1* direction than observed. This model also predicts smaller $V_N$ and $V_T$ components at *V2* than observed and predicts $V_N > V_T$, opposite of observations.

Provornikova et al. (2014) use Interplanetary Scintillation (IPS) data as input for a 3D time-dependent heliosphere model. The time-dependent model predicts the *V2* $V_R$ is slightly higher than observed and a *V1* $V_R$ 100 km s$^{-1}$ greater than observed. This model matches the *V1* $V_T$ values well, but significantly underestimates *V2* $V_T$ and overestimates *V2* $V_N$. Thus neither model fits either *V1* or *V2* observations, and *V1* and *V2* flows look very different.

## 4. SUMMARY

*Voyager 2* has sampled the heliosheath for 20 AU. The plasma data are of good quality, although as the plasma turns tailward larger portions of the plasma distribution cannot be observed. The speed has remained constant across the heliosheath, a surprise. $V_R$ has decreased, but $V_T$ and $V_N$ have increased to keep the speed constant. The flow is turning faster in the T than N directions, with a flow angle of about 60° from radial in the

RT plane and 30° from radial in the RN plane. The average density has remained constant since an increase in 2011; the thermal speed is also not changing. The *V2* flows are very different than those at *V1* derived from LECP data. However, comparison of plasma and LECP flows derived at *V2* usually show similar velocities, so we do not think the *V1* differences are instrumental. Models also have trouble replicating these data; clearly something is missing from our physical picture of these flows.

## REFERENCES

Bridge, H. S., Belcher, J. W., Butler, R. J., et al. 1977, SSRv, 21, 259
Burlaga, L. F., & Ness, N. F. 2009, ApJ, 703, 311
Burlaga, L. F., Ness, N. F., Gurnett, D. A., & Kurth, W. S. 2013, ApJL, 778, L3
Burlaga, L. F., Ness, N. F., & Stone, E. C. 2013, Sci, 341, 147
Decker, R. B., Krimigis, S. M., Roelof, E. C., et al. 2003, AdSpR, 32, 591
Decker, R. B., Krimigis, S. M., Roelof, E. C., et al. 2005, Sci, 309, 2020
Decker, R. B., Krimigis, S. M., Roelof, E. C., & Hill, M. E. 2010, in AIP Conf. Proc. 1302 Pickup Ions Throughout the Heliosphere and Beyond, ed. J. A. Le Roux et al. (Melville, NY: AIP), 51
Fisk, L. A., & Gloeckler, G. 2009, AdSpR, 43, 1471
Fisk, L. A., & Gloeckler, G. 2013, AGU Fall Meeting SH14B-06 (Washington, DC: AGU)
Gleeson, L. J., & Axford, W. F. 1968, Ap&SS, 2, 431
Gurnett, D. A., Kurth, W. S., Burlaga, L. F., & Ness, N. F. 2013, Sci, 341, 1489
Krimigis, S. M., Roelof, E. C., Decker, R. B., & Hill, M. E. 2011, Natur, 474, 359
Krimigis, S. M., Carbary, J. F., Keath, E. P., et al. 1981, JGR, 86, 8227
Krimigis, S. M., Decker, R. B., Roelof, E. C., et al. 2013, Sci, 341, 144
Pogorelov, N. V., Suess, S. T., Borovikov, S. N., et al. 2013, ApJ, 772, 2
Provornikova, E., Opher, M., Izmodenov, V. V., et al. 2014, ApJ, in press
Richardson, J. D. 2011, ApJ, 740, 113
Richardson, J. D., & Wang, C. 2012, ApJL, 759, L19
Stone, E. C., Cummings, A. C., McDonald, F. B., et al. 2013, Sci, 341, 150
Webber, W. R., & McDonald, F. B. 2013, GeoRL, 40, 1665